Development of Wireless Communicator for Receiver Current Phase Control in 6.78MHz Resonant Inductive Coupling Wireless Power Transfer

Kairi Kato
Graduate school of environment, life, natural science and technology
Okayama University
Okayama, Japan
ppjk8tyf@s.okayama-u.ac.jp

Masataka Ishihara
Graduate school of environment, life, natural science and technology
Okayama University
Okayama, Japan
masataka.ishihara @okayama-u.ac.jp

Kazuhiro Umetani
Faculty of Information Science and Electric Engineering.
kyushu University
Fukuoka, Japan
umetani@eec.kyushu-u.ac.jp

Eiji Hiraki
Graduate school of environment, life, natural science and technology
Okayama University
Okayama, Japan
hiraki @okayama-u.ac.jp

***Abstract*— Recently, resonant inductive coupling wireless power transfer (RIC-WPT) systems operating at 6.78 MHz for charging mobile and consumer electronic devices placed in a wide area have attracted researchers' attention. In RIC-WPT systems, methods employing reactance compensators utilizing semiconductor switches have been proposed to match the resonant frequencies between the transmitter and receiver. To implement such a reactance compensator on the receiver side, synchronization between the transmitter and receiver control signals is required. In other words, a constant phase difference must be maintained between the control signal on the transmitter side and that on the receiver side. Therefore, this study presents the development of a radio frequency (RF) wireless communication method for the receiver side control in a 6.78 MHz RIC-WPT system. The communication system adopts quadrature demodulation and a phase-locked loop to maintain a constant phase difference between the transmitted reference signal and the demodulated signal. The experimental results indicate that the output power fluctuation caused by the developed communication circuit is expected to be less than 10%, suggesting its potential applicability to 6.78 MHz RIC-WPT systems.**

Keywords—resonant inductive coupling wireless power transfer, cross-coupling, reactance compensator, phase-synchronization, wireless communication

I. INTRODUCTION

In recent years, wireless power transfer (WPT) technology has been attracting attention from the viewpoint of safety and convenience because WPT technologies can transfer electric power without physical cable connections. An example of an application of this technology is the wireless power transfer desk, as illustrated in Fig. 1. This system enables the wireless charging of electronic devices such as smartphones placed on the desk. In addition, WPT can be applied to a wide range of applications, including biomedical implants and wearable devices [1].

Among various types of the WPT technique, the resonant inductive coupling wireless power transfer (RIC-WPT) is promising in applications such as that shown in Fig. 1 due to its relatively high efficiency and capability to cover a wider area [2]–[5]. For applications that require relatively compact receivers and a wide power transfer area, the 6.78 MHz frequency, which belongs to the ISM (industrial, scientific, and medical) band, is widely used [2][3]. Fig. 2 shows a typical RIC-WPT system. Both the transmitter and receiver are equipped with LC resonators, and their resonance frequencies are generally designed to be close to the operating frequency. Therefore, the inverter can output the large ac current to the transmitter coil and this current can further

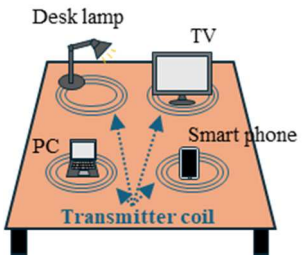

Fig. 1. Wireless charging desk

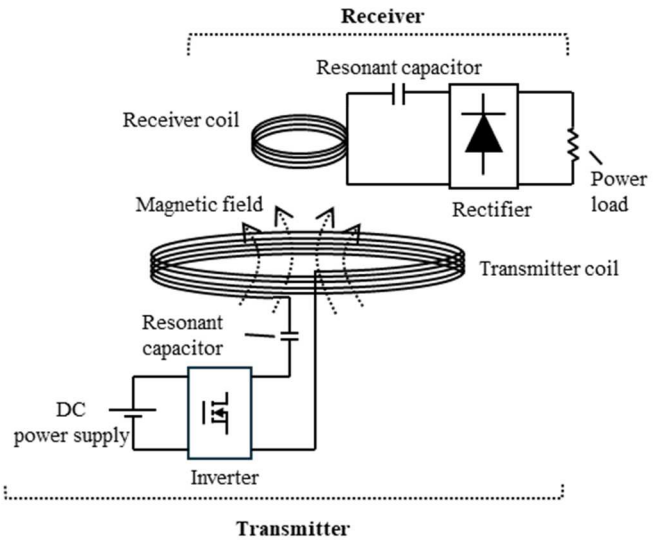

Fig. 2. RIC-WPT system

induce large resonant current effectively in the receiver resonators.

However, the RIC-WPT systems often suffer from resonance frequency deviation, leading to a reduction in power and efficiency [6][7]. One of these factors is the manufacturing tolerance and aging of the coil and the resonant capacitor. In practical mass production of resonators, individual fine-tuning of the resonance frequency is generally unrealistic. Therefore, parameter tolerances become a critical issue. Another is mutual interference in the case of multiple transmitters and receivers. These effectively lead to deviations in the resonance frequency.

To address this issue, an automatic resonant frequency tuning system has been proposed. Resonant frequency compensation is typically implemented using a variable reactance. In recent years, various methods have been proposed for realizing variable reactance, including capacitor matrices [8], DC voltage-controlled variable capacitors [9], gate-controlled series capacitors [10], capacitors controlled by stepping motors [11], DC current-controlled inductors [12], active rectifier [13][14] and automatic tuning assist circuits (ATAC) [15][16]. Among these methods, the ATAC and active rectifier have the potential to outperform others, as it can automatically adjust its reactance with only simple control. This paper assumes a system equipped with the ATAC as a basis for the following discussion.

Fig. 3 shows the operating principle of the ATAC. As shown in Fig. 3, the ATAC consists of a half-bridge circuit and a smoothing capacitor, and ideally, it has no resistive components. Therefore, under steady-state conditions, the ATAC does not receive any effective power, and its output voltage must be orthogonal to the resonant current. In other words, the ATAC can adjust the phase of the resonant current according to its output voltage phase [7]. When the ATAC is installed on the transmitter side, controlling the resonant current is relatively straightforward, as the reference signal can be delivered via a wired connection. However, when the ATAC is installed on the receiver side, the challenge lies in how to obtain the driving signal. Since the phase of the resonant current is controlled by the output voltage phase of the ATAC, the phase difference between the driving signal of the ATAC and the reference signal must remain constant at all times. This requirement represents a major concern when implementing the ATAC on the receiver side. Hereafter, the condition that the phase difference between the two signals remains constant is referred to as phase synchronization in this paper.

Various phase synchronization methods have been proposed for controlling the phase of the receiver-side current. First, a method for generating the drive signal of the phase-controlled reactance compensator (e.g., ATAC) from the receiver current has been proposed [17]-[19]. This method eliminates the need for wireless communication; however, it has not yet been demonstrated at high frequencies such as 6.78 MHz. This is likely because accurately detecting the zero-crossing point of the current waveform becomes increasingly difficult at such frequencies. Second, a method that obtains the phase information of the transmitter-side current using an auxiliary coil has been proposed [20][21]. In such systems, the auxiliary coil must be decoupled from the receiver coil. However, if the coupling coefficient between the receiver coil and the auxiliary coil varies, mutual interference may occur, which causes inaccurate phase synchronization. Third, a

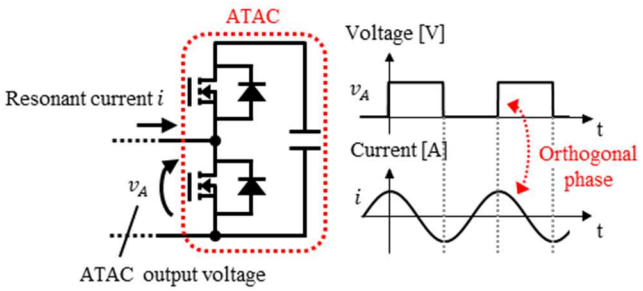

Fig.3. Operating principle of the ATAC

method that transmits the reference signal using wireless communication has been proposed [22]-[24]. [22] proposed an approach using infrared signals. However, infrared communication may suffer from a limited communication area due to its high directionality and susceptibility to obstruction. [23] proposed a synchronization method in which a 433.92 MHz continuous wave tone is transmitted to both transmitter and receiver sides and frequency division is used to synchronize the frequency. In [24], a phase synchronization technique utilizing ultra-wideband (UWB) was proposed, which is considered to perform synchronization at regular intervals. The methods presented in [23] and [24] are considered promising for phase synchronization in RIC-WPT systems, as they can be applied at high frequencies and are support relatively wide communication area. However, since [23] does not employ modulation, it may lack robustness in communication, and because [24] does not achieve synchronization of continuous signals, there is a possibility of phase drift occurring during the synchronization interval.

Therefore, this paper presents the development of a wireless communication circuit aimed at achieving accurate phase synchronization by modulating a continuous signal and transmitting it, as one of the methods to enable receiver current control in a 6.78 MHz RIC-WPT system. Since this wireless communication uses radio waves, it offers a relatively wide communication area, thereby not limiting the power transmission area.

The remainder of this paper comprises four sections. Section II presents an overview of the RIC-WPT system considered in this paper. Section III describes the wireless communication circuit designed to achieve phase synchronization. Section IV reports experimental results on the phase fluctuation of the wireless communication circuit and its impact on the output power of the WPT system. Finally, Section V concludes the paper.

II. RIC-WPT System Incorporating Wireless Communication

This section describes the RIC-WPT system considered in this paper and quantifies the variation in output power caused by phase variation in wireless communication.

A. Overview of the considered RIC-WPT system

Fig.4 shows the configuration of the RIC-WPT system. This system incorporates the ATAC on both the transmitter and the receiver sides. $\boldsymbol{V_A}$ denotes the output voltage of the ATAC incorporated in the receiver, $\boldsymbol{I_r}$ is the receiver current. In this system, the receiver ATAC signal from is wirelessly transmitted from the transmitter.

The operation of ATAC at the receiver side is briefly described below. As shown in Fig.4 the ATAC consists of two

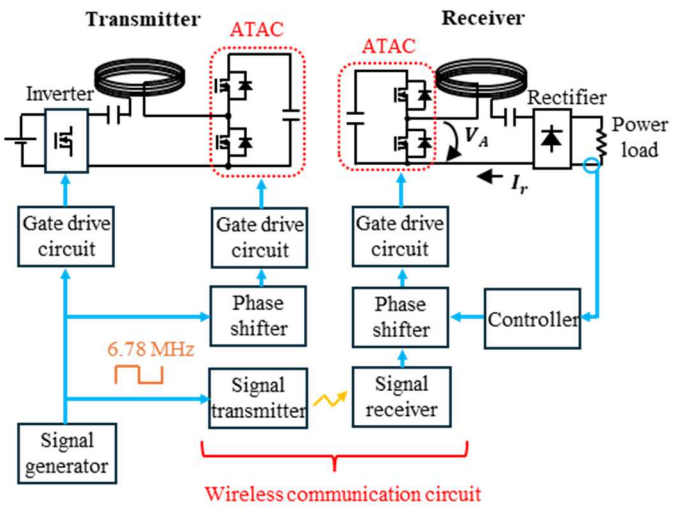

Fig.4. Diagram of the considered RIC-WPT system

semiconductor switches and one capacitor, and is designed not to receive active power. Therefore, the ATAC voltage $\boldsymbol{V_A}$ and the current $\boldsymbol{I_r}$ are orthogonal. This property enables the ATAC to control the phase of $\boldsymbol{I_r}$ by adjusting the phase of the gate signal.

In this system, the phase of the ATAC gate signal is controlled using a hill-climbing algorithm, based on the implementation in [22]. This algorithm incrementally adjusts the phase difference while monitoring output power, automatically converging to the optimal phase that maximizes output power. Although this method is unaffected by constant phase offsets caused by transmission delay in the wireless communication link, it becomes sensitive to variations in the delay. Such variations can destabilize the phase difference, making it difficult for the system to reach the point of maximum output power. To address this issue, a wireless phase-synchronized communication system that maintains a constant phase difference between transmitted and received waveforms is required.

B. Effects of Phase Variations in Wireless Communication

Phase variation in wireless communication should be limited to maintain the output power variation within a target range (e.g., 10%) as a design guideline. As an evaluation metric, the output power variation due to phase variation is calculated. Fig.5(a) shows the equivalent circuit of the receiver, and Fig.5(b) shows the corresponding phasor diagram. For simplifying the discussion, harmonic components in the resonant currents and voltage are assumed to be negligible compared to the fundamental component, and both the induced electromotive force and the ATAC are modeled as equivalent AC voltage sources. Here, r_r is the parasitic resistance of the receiver coil; L_r is its self-inductance; C_r is the capacitance of the resonant capacitor; R_L is the equivalent load resistance; M is the mutual inductance between the transmitter and receiver coils; $\boldsymbol{I_t}$, $\boldsymbol{I_r}$ and $\boldsymbol{V_A}$ represent the transmitter current, the receiver current, and ATAC output voltage, respectively; I_t, I_r and V_A represent the RMS values of $\boldsymbol{I_t}$, $\boldsymbol{I_r}$ and $\boldsymbol{V_A}$, respectively. As shown in Fig.5 (b), θ is the phase difference between $\boldsymbol{V_A}$ and $\boldsymbol{I_t}$. While the influence of the receiver current on the transmitter should be considered, the transmitter current is assumed constant for simplification in this analysis.

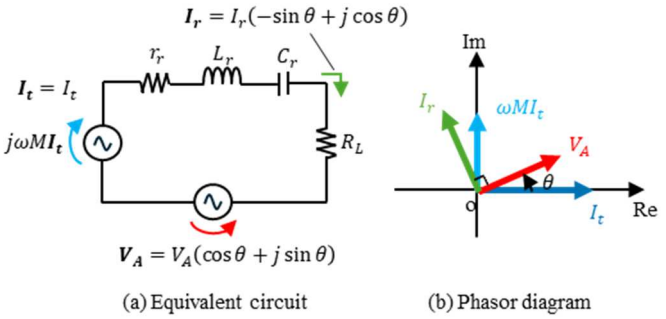

Fig.5.Equivalent circuit and phasor diagram of the receiver

By applying Kirchhoff's laws to Fig.5 and separating the real and imaginary components, the following equations are obtained.

$$0 = -\left\{(r_r + R_L)\sin\theta + \left(\omega L_r - \frac{1}{\omega C_r}\right)\cos\theta\right\} I_r + V_A\cos\theta \quad (1)$$

$$\omega M I_t = \left\{(r_r + R_L)\cos\theta - \left(\omega L_r - \frac{1}{\omega C_r}\right)\sin\theta\right\} I_r + V_A\sin\theta \quad (2)$$

By eliminating V_A from (1) and (2), I_r can be expressed as follows:

$$I_r = \frac{\omega M I_t \cos\theta}{r_r + R_L} \quad (3)$$

The output power P_o can be calculated as follows:

$$P_o = R_L I_r^2 = R_L\left(\frac{\omega M I_t\cos\theta}{r_r + R_L}\right)^2 \quad (4)$$

The maximum output power $P_{o\,max}$ is achieved when $\theta = 0°$, and is given by:

$$P_{o\,max} = R_L\left(\frac{\omega M I_t}{r_r + R_L}\right)^2 \quad (5)$$

Next, the range of θ satisfying $P_o \geq \alpha P_{o\,max}$ is derived, where $0 < \alpha \leq 1$. The corresponding condition is given by:

$$\frac{P_o}{P_{omax}} = \cos^2\theta \geq \alpha \quad (6)$$

The range of θ that satisfies (6) is given by:

$$-\cos^{-1}(\sqrt{\alpha}) \leq \theta \leq \cos^{-1}(\sqrt{\alpha}) \quad (7)$$

To limit the output power reduction to less than 10%, α is set to 0.9, and thus (7) becomes:

$$-18.4° \leq \theta \leq 18.4° \quad (8)$$

A constant deviation of 18.4° from the optimal value of θ results in a 10% reduction in output power. This value can be used as an indicator for evaluating phase variations in wireless communication circuits.

III. Phase-Synchronized Wireless Communication System

This section describes the configuration of the wireless communication system and how it achieves phase synchronization.

A. Configuration of the Wireless Communication System

Fig.6 shows the configuration of the proposed wireless phase-synchronized communication system. First, a 6.78 MHz signal used by the inverter on the transmitter side is generated by a signal generator. This signal is multiplied with a carrier wave using a mixer, amplified by a power amplifier, and then transmitted through an antenna. The receiver captures the transmitted wave via its antenna, amplifies the received signal, and demodulates it. To avoid frequency offset, the system multiplies the modulated signal with in-phased (I)

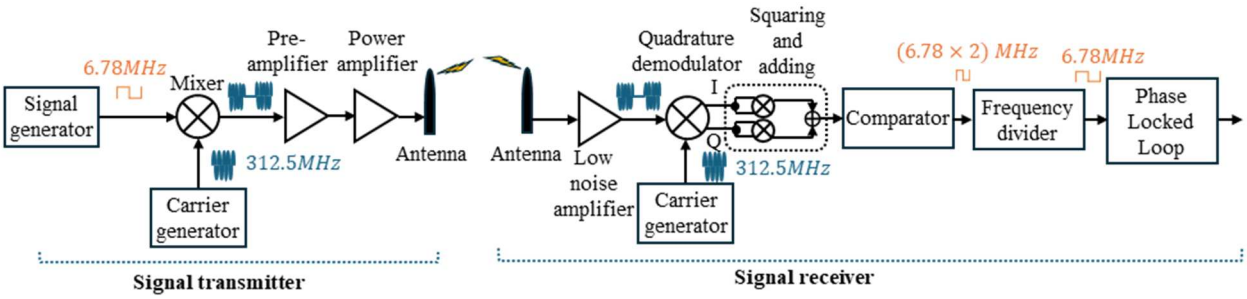

Fig.6. Diagram of wireless communication circuit

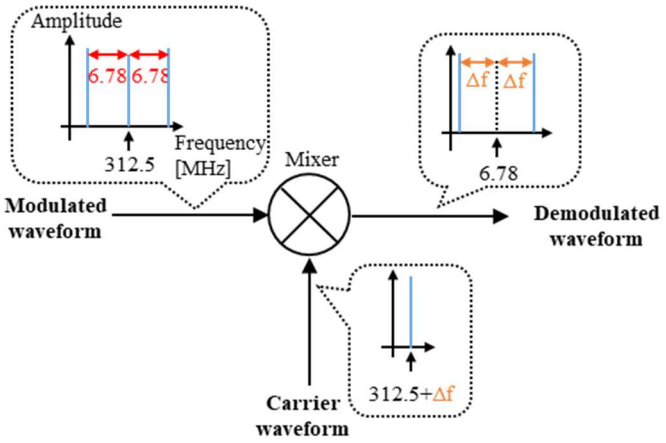

Fig.7. Frequency spectrum without quadrature demodulation

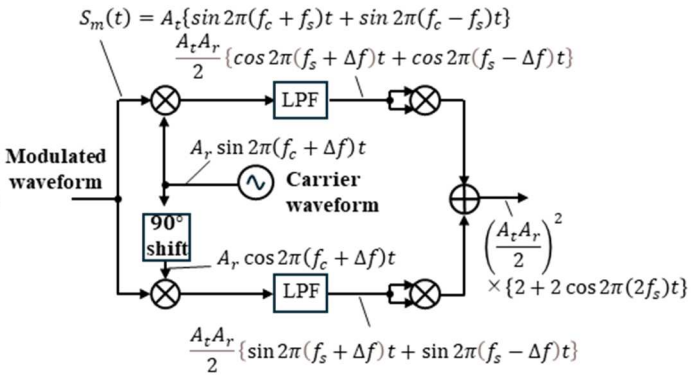

Fig.8. Diagram of quadrature demodulation circuit

and quadrature (Q) carrier waves. The resulting two signals are squared individually and then summed. A comparator is then used to convert the summed signal into a square wave by comparing it with its average value. Since the quadrature demodulation involves squaring, the signal frequency doubles. A frequency divider is therefore employed to halve the frequency, producing a 6.78 MHz square wave. Finally, a Phase-Locked Loop (PLL) is used at the final stage to suppress phase fluctuations, completing the demodulation process.

B. Role of Quadrature Demodulation

The reason for employing quadrature demodulation in this system is to eliminate frequency offset between the baseband signal (a 6.78 MHz square wave generated on the transmitter side) and the demodulated waveform. Fig.7 shows the frequency spectrum when demodulation is performed without using a quadrature demodulator. In general, the carrier signals at the transmitter and receiver are generated independently, which causes a slight frequency offset, denoted as Δf. When demodulation is performed by directly multiplying the received signal with the local carrier in the presence of Δf, the resulting waveform is shifted by Δf from the baseband frequency. Fig.8 illustrates the structure of the quadrature demodulator. The modulated signal $S_m(t)$ is assumed to be represented by the following equation.

$$S_m(t) = A_t\{sin\,2\pi(f_c + f_s)t + sin\,2\pi(f_c - f_s)t\} \quad (9)$$

Here, A_t denotes the amplitude of the modulated signal, f_c is the carrier frequency at the transmitter, and f_s is the baseband signal frequency (6.78 MHz in this case). For simplicity, phase differences are neglected. The modulated signal is multiplied by the carrier and a carrier shifted by 90° in phase, as shown in Fig.8. After passing through a low-pass filter to re move unwanted high-frequency components, two signals expressed by the following equations are obtained.

$$\frac{A_tA_r}{2}\{cos\,2\pi(f_s + \Delta f)t + cos\,2\pi(f_s - \Delta f)t\} \quad (10)$$

$$\frac{A_tA_r}{2}\{\sin 2\pi(f_s + \Delta f)t + \sin 2\pi(f_s - \Delta f)t\} \quad (11)$$

At this stage, the effect of frequency offset in the carrier remains; however, squaring and summing these two signals yields the following expression.

$$\left(\frac{A_tA_r}{2}\right)^2\{2 + 2\cos 2\pi(2f_s)t\} \quad (12)$$

From (12), only the frequency component at twice the baseband frequency f_s is extracted. By removing the DC component of this signal and applying it to a frequency divider in the subsequent stage, the f_s component can be successfully demodulated.

C. Role of the Phase-Locked Loop (PLL)

The reason for incorporating a Phase-Locked Loop (PLL) at the final stage of the receiver is to further suppress phase fluctuations. In general, during quadrature demodulation, errors can occur due to limitations in IC precision when multiplying the modulated signal by orthogonal carrier waves. These errors result in residual phase variations, which the PLL is designed to reduce. Fig.9 illustrates the principle by which the PLL suppresses phase fluctuations. When the phase of the input signal to the PLL varies, the pulse width of the output from the phase detector increases. Although this leads to an attempt to increase the output of the loop filter, the filter is designed with a cutoff frequency lower than frequency of the phase variation, so its output remains nearly constant. Consequently, the output frequency of the voltage-controlled oscillator (VCO) remains stable, and phase fluctuations are effectively suppressed.

IV. EXPERIMENT

In this section, we experimentally evaluate the phase fluctuations of the fabricated wireless communication circuit. Table I lists the experimental instruments used in this study. Fig.10 shows a prototype of the developed circuit. For the quadrature demodulator, we used the DC1670A evaluation board, which incorporates the LTC5584 from Analog Devices. First, we observed the output of this evaluation kit. Fig.11 shows the in-phase (I) and quadrature (Q) components. As seen in the figure, the waveforms exhibit a beat frequency of approximately 2 kHz, which results from the frequency offset between the transmitter and receiver carrier signals and corresponds to Δf in Fig. 8. If these signals are directly connected to a comparator to generate square waves, the phase continues to drift due to the frequency difference. Furthermore, examining the phase difference between the I and Q components reveals that, ideally, they should be orthogonal; however, the beat signals are not perfectly orthogonal and exhibit a phase difference of approximately 106°. As a result, when the I and Q signals are squared and summed, the beat component is not completely canceled, leading to residual phase fluctuations.

Fig.12 shows the baseband signal, the demodulated waveform without the PLL, and the demodulated waveform with the PLL. In this experiment, the PLL loop filter was implemented using an RC low-pass filter with a time constant of 100 seconds. As seen in Fig. 12, demodulation is achieved at nearly the same frequency, but phase difference variations cannot be observed. To obtain a more precise understanding of the phase variation and observe its long-term trend, Fig.13 presents bar graphs of the phase difference in each period. Note that due to the resolution of the oscilloscope, the sampling period is 1.6 ns (equivalent to 3.9° at 6.78 MHz), and thus the measured phase difference should be considered as a reference only. Fig.13(a) shows that, without the PLL, the phase difference varies periodically, which is considered to be determined by the frequency offset between the carrier signals. In contrast, Fig.13(b) demonstrates that the phase variation is suppressed by the PLL. Experimental results indicate a phase fluctuation of approximately 46.9° without the PLL and about 15.6° with the PLL.

rom (6), the output power of the WPT system with a phase variation of 15.6° is estimated to be 92.7 % of the maximum value, showing that the output power remains within an acceptable range.

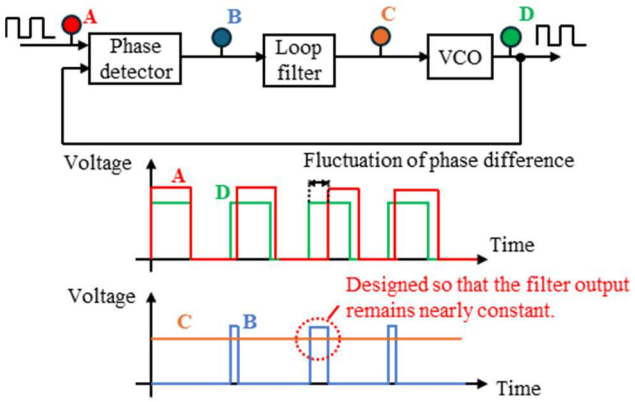

Fig.9. Operation of PLL

Table I. List of experimental instruments

Instrument	Model Number (Manufacturer)
Oscilloscope	MSO44, (Tektoronix)
Probe	TPP0500B, (Tektoronix)
Function Generator	WF1943 , (NF)

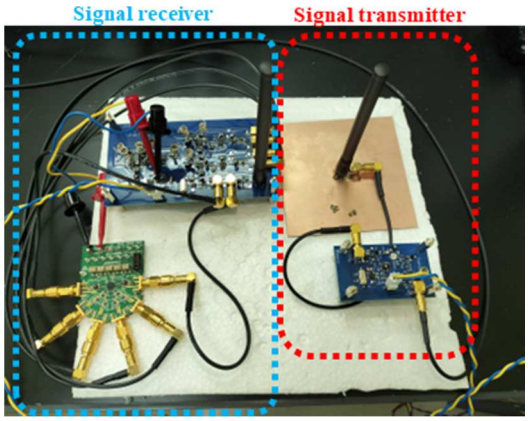

Fig.10. Prototype of wireless communication circuit

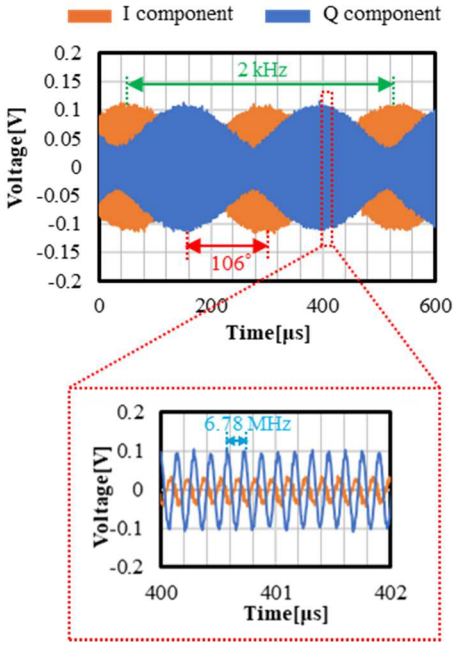

Fig.11. In-phase and Quadrature component

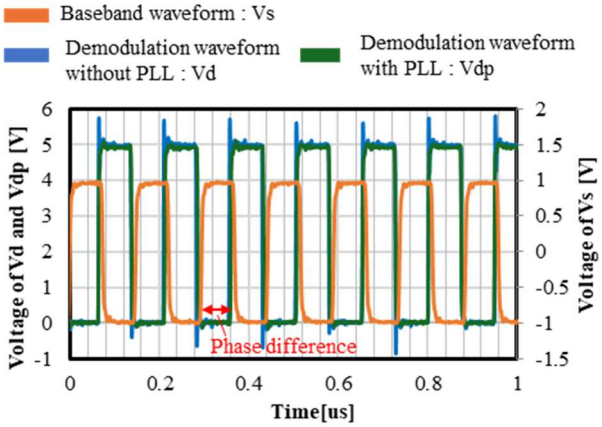

Fig.12. Diagram of quadrature demodulation circuit

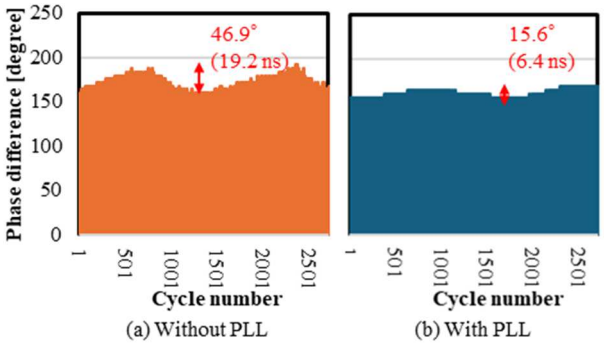

Fig.13. Phase difference between baseband waveform and demodulation waveform

V. CONCLUSIONS

This paper developed a wireless phase synchronization method for applying adaptive tuning using an ATAC to a 6.78 MHz RIC-WPT system. A radio frequency (RF) communication circuit combining quadrature demodulation and PLL was implemented to transmit the control reference signal from the transmitter to the receiver. Experimental results demonstrated that the proposed communication system achieved a phase fluctuation of approximately 15.6°, resulting in an output power level exceeding 92.7% of the maximum value. These results confirm the feasibility of applying RF-based wireless phase synchronization to high-frequency WPT systems.

REFERENCES

[1] Y. -J. Kim, D. Ha, W. J. Chappell and P. P. Irazoqui, "Selective Wireless Power Transfer for Smart Power Distribution in a Miniature-Sized Multiple-Receiver System," in IEEE Transactions on Industrial Electronics, vol. 63, no. 3, pp. 1853-1862, March 2016.

[2] M. Fu, Z. Tang and C. Ma, "Analysis and Optimized Design of Compensation Capacitors for a Megahertz WPT System Using Full-Bridge Rectifier," in IEEE Transactions on Industrial Informatics, vol. 15, no. 1, pp. 95-104, Jan. 2019.

[3] L. Jiang and D. Costinett, "A High-Efficiency GaN-Based Single-Stage 6.78 MHz Transmitter for Wireless Power Transfer Applications," in IEEE Transactions on Power Electronics, vol. 34, no. 8, pp. 7677-7692, Aug. 2019.

[4] J. Song, M. Liu and C. Ma, "Analysis and Design of a High-Efficiency 6.78-MHz Wireless Power Transfer System With Scalable Number of Receivers," in IEEE Transactions on Industrial Electronics, vol. 67, no. 10, pp. 8281-8291, Oct. 2020.

[5] F. Liu, K. Li, K. Chen and Z. Zhao, "A Phase Synchronization Technique Based on Perturbation and Observation for Bidirectional Wireless Power Transfer System," in IEEE Journal of Emerging and Selected Topics in Power Electronics, vol. 8, no. 2, pp. 1287-1297, June 2020.

[6] K. Matsuura, M. Ishihara, A. Konishi, K. Umetani and E. Hiraki, "Multiple-Transmitter Achieving Load-Independent Transmitter Current and Compensation of Cross-Interference Among Transmitters for Wide Charging Area Wireless Power Transfer Systems," 2020 IEEE Energy Conversion Congress and Exposition (ECCE), Detroit, MI, USA, 2020.

[7] M. Ishihara, K. Fujiki, K. Umetani and E. Hiraki, "Automatic Active Compensation Method of Cross-Coupling in Multiple-receiver Resonant Inductive Coupling Wireless Power Transfer Systems," 2019 IEEE Energy Conversion Congress and Exposition (ECCE), Baltimore, MD, USA, 2019.

[8] Q. Wang and Y. Wang, "Power efficiency optimisation of a three-coil wireless power transfer using compensatory reactance," IET Power Electron., vol. 11, no. 13, pp. 2102–2108, Nov. 2018.

[9] J. Tian and A. P. Hu, "A DC-Voltage-Controlled Variable Capacitor for Stabilizing the ZVS Frequency of a Resonant Converter for Wireless Power Transfer," in IEEE Transactions on Power Electronics, vol. 32, no. 3, pp. 2312-2318, March 2017

[10] J. Osawa, T. Isobe, and H. Tadano, "Efficiency improvement of high frequency inverter for wireless power transfer system using a series reactive power compensator," in Proc. IEEE Power Electron. Drive Syst. Conf. (PEDS2017), Honolulu, HI, USA, 2017, pp. 992–998.

[11] A. Trigui, S. Hached, F. Mounaim, A. C. Ammari and M. Sawan, "Inductive Power Transfer System With Self-Calibrated Primary Resonant Frequency," in IEEE Transactions on Power Electronics, vol. 30, no. 11, pp. 6078-6087, Nov. 2015.

[12] S. Aldhaher, P. C. -K. Luk and J. F. Whidborne, "Electronic Tuning of Misaligned Coils in Wireless Power Transfer Systems," in IEEE Transactions on Power Electronics, vol. 29, no. 11, pp. 5975-5982, Nov. 2014.

[13] A. Berger, M. Agostinelli, S. Vesti, J. A. Oliver, J. A. Cobos and M. Huemer, "A Wireless Charging System Applying Phase-Shift and Amplitude Control to Maximize Efficiency and Extractable Power," in IEEE Transactions on Power Electronics, vol. 30, no. 11, pp. 6338-6348, Nov. 2015.

[14] K. Colak, E. Asa, M. Bojarski, D. Czarkowski and O. C. Onar, "A Novel Phase-Shift Control of Semibridgeless Active Rectifier for Wireless Power Transfer," in IEEE Transactions on Power Electronics, vol. 30, no. 11, pp. 6288-6297, Nov. 2015.

[15] Y. Endo and Y. Furukawa, "Proposal for a new resonance adjustment method in magnetically coupled resonance type wireless power transmission," 2012 IEEE MTT-S International Microwave Workshop Series on Innovative Wireless Power Transmission: Technologies, Systems, and Applications, Kyoto, Japan, 2012

[16] M. Ishihara, K. Umetani and E. Hiraki, "Impedance Matching to Maximize Induced Current in Repeater of Resonant Inductive Coupling Wireless Power Transfer Systems," 2018 IEEE Energy Conversion Congress and Exposition (ECCE), Portland, OR, USA, 2018.

[17] K. Matsuura, D. Kobuchi, Y. Narusue and H. Morikawa, "Communication-Less Receiver-Side Resonant Frequency Tuning for Magnetically Coupled Wireless Power Transfer Systems," in IEEE Access, vol. 11, pp. 23544-23556, 2023.

[18] D. Zhang, M. Chen, B. Li, X. Wang, X. Sun and F. Jiang, "Synchronization Strategy Based on Resonant Current Detection for Bidirectional Wireless Charging System," in IEEE Transactions on Power Electronics, vol. 37, no. 9, pp. 11436-11449, Sept. 2022.

[19] S. Jia, C. Chen, P. Liu and S. Duan, "A Digital Phase Synchronization Method for Bidirectional Inductive Power Transfer," in IEEE Transactions on Industrial Electronics, vol. 67, no. 8, pp. 6450-6460, Aug. 2020.

[20] D. J. Thrimawithana, U. K. Madawala, and M. Neath, "A synchronization technique for bidirectional IPT systems," IEEE Trans. Ind. Electron., vol. 60, no. 1, pp. 301–309, Jan. 2013

[21] R. Mai, Y. Liu, Y. Li, P. Yue, G. Cao and Z. He, "An Active-Rectifier-Based Maximum Efficiency Tracking Method Using an Additional Measurement Coil for Wireless Power Transfer," in IEEE Transactions on Power Electronics, vol. 33, no. 1, pp. 716-728, Jan. 2018.

[22] A. Konishi, K. Umetani, M. Ishihara and E. Hiraki, "Autonomous resonant frequency tuner for a 6.78MHz inductive coupling wireless power transfer system to stably maximize repeater current", IEEJ J. Ind. Appl., vol. 12, no. 2, pp. 215-227, Mar. 2023.

[23] N. Pucci, J. M. Arteaga, C. H. Kwan, D. C. Yates and P. D. Mitcheson, "A 13.56 MHz Bidirectional IPT System with Wirelessly Synchronised Transceivers for Ultra-Low Coupling Operation," 2021 IEEE Energy Conversion Congress and Exposition (ECCE), Vancouver, BC, Canada, 2021, pp. 5781-5787.

[24] W. Ye, P. Shukla and N. Parspour, "Ultra-Wideband Based Synchronization Method for Bidirectional Wireless Power Transfer Systems," 2025 IEEE Wireless Power Technology Conference and Expo (WPTCE), Rome, Italy, 2025, pp. 1-5.